AUTHOR QUERIES

AUTHOR PLEASE ANSWER ALL QUERIES

PLEASE NOTE: We cannot accept new source files as corrections for your paper. If possible, please annotate the PDF proof we have sent you with your corrections and upload it via the Author Gateway. Alternatively, you may send us your corrections in list format. You may also upload revised graphics via the Author Gateway.

AQ:1 = Author: Please confirm or add details for any funding or financial support for the research of this article.
AQ:2 = Please confirm whether the e-mail address of the authors Birudula Anil Kumar and Raghu Selvaraj are correct as set.
AQ:3 = Please provide the department name for Indian Maritime University where the author U. S. Ramesh was affiliated with.
AQ:4 = Fig. 3 should be cited before Fig. 4. Please update the in-text citations.
AQ:5 = Please specify the reference number for the author "BØ" in the sentence beginning with "examined multiple fixed speed DEG system..."
AQ:6 = Please provide the expansion for ADC and GHG.
AQ:7 = Please provide the accessed date for Refs. [10] and [55].
AQ:8 = Please provide the author names for Ref. [23].
AQ:9 = Please provide the organization location and report no. for Ref. [39].
AQ:10 = Please provide the organization name, organization location, and report no. for Ref. [42].
AQ:11 = Please provide the city name for National Institute of Ocean Technology, THDC India Limited, Central Power Research Institute, National Mission on Power Electronics Technology, and Ministry of Shipping.

Improved Fuel-Use Efficiency in Diesel–Electric Tugboats With an Asynchronous Power Generating Unit

Birudula Anil Kumar, *Student Member, IEEE*, Raghu Selvaraj, *Student Member, IEEE*, and Thanga Raj Chelliah, *Senior Member, IEEE*, and U. S. Ramesh

***Abstract*— High capacity diesel–electric tugboats are employed at every modernized harbor for assisting big marine vessels and other harbor applications. Contemporary tugboats use multiple power sources to meet their propulsion and auxiliary on-board load demands. The effective utilization of multiple power sources leads to better fuel use efficiency with reduced emissions, economic, and environmental benefits. This paper presents a simple optimization technique for scheduling available power sources of a diesel–electric tugboat [diesel engine generators (DEGs) and batteries] to meet its load demand with an objective to minimize fuel consumption. For this paper, a diesel–electric tugboat system of 1.1-MW capacity with different generating systems is considered: 1) fixed speed generating unit (2 × 550 kW fixed speed DEG employing synchronous generators) and 2) variable speed generating unit [1 × 1.1 MW variable speed DEG employing doubly fed induction generator (DFIG)]. From the optimized test results, it is inferred that the variable speed generating unit offers a fuel saving of 29.86% in comparison with diesel-mechanical propelled system and 2.9% in comparison with fixed speed diesel–electric system. The simulation of a 1.1-MW variable speed generating system is performed in MATLAB/Simulink 2014A environment, and experimental demonstration is performed through a 2.2-kW laboratory prototype.**

***Index Terms*— Diesel engine generators (DEGs), doubly fed induction generator (DFIG), energy storage systems (ESSs), optimization, power management, tugboat.**

Nomenclature

I_{dL}, I_{qL}	d-axis and q-axis load side current, respectively.
$I_{dr} I_{qr}$	d-axis and q-axis machine side current, respectively.
$V_{dL} V_{qL}$	d-axis and q-axis load side voltage, respectively.
$V_{dr} V_{qr}$	d-axis and q-axis machine side voltage, respectively.
T_e	Electromagnetic torque.
V_{dc}	DC-link voltage.
θ_s, θ_r	Stator angle, rotor angle, respectively.
Q_s, Q_L	Stator and load reactive power, respectively.
ω_s, ω_r	Stator and rotor angular frequency, respectively.
i_{ms},	Magnetizing current.
Ψ_s	Stator flux.

AQ:1 Manuscript received January 28, 2019; accepted March 6, 2019. This work was supported by the Ministry of Shipping, Government of India vide under Grant MSR-912-WRC (2016–2019). *(Corresponding author: Birudula Anil Kumar.)*

B. A. Kumar and T. R. Chelliah are with the Hydropower Simulation Laboratory, Department of Water Resources Development and Management, IIT Roorkee, Roorkee 247 667, India (e-mail: banil1109@gmail.com; thangfwt@iitr.ac.in). AQ:2

R. Selvaraj is with the Power Electronics and Hydro-Electric Machines Laboratory, Department of Water Resources Development and Management, IIT Roorkee, Roorkee 247 667, India (e-mail: raghu.selvaraj89@gmail.com).

AQ:3 U. S. Ramesh is with the Indian Maritime University, Visakhapatnam Campus, Visakhapatnam 530 011, India (e-mail: usramesh@imu.ac.in).

Digital Object Identifier 10.1109/TTE.2019.2906587

I. Introduction

In MARINE industry, tugboats are employed in harbors for maneuvering big vessels, firefighting, water patrolling, and ice breaking. The intervention of key enabling technologies has transitioned marine vessel architecture from steam engines to diesel engine generator (DEG) in view of better efficiency and reliability with reduced operational cost, and quick start capability [1]–[4]. The first diesel engine (DE) invented by Rudolf Diesel had a drawback of nonreversibility which made them impractical for marine applications. Later, the invention of double camshaft, mechanical clutches, and reversing gears made DE feasible in marine applications [5]. In 1903, the first diesel–electric propelled Russian vessel "Vandal" was constructed in the yards of Nobel Brothers Company, San Petersburg with three sets of 120-hp DE (each DE is coupled with 87-kW generator) for feeding electric propulsion [6]. Later in 1954, Wasmund [4] discussed the use of multiple electrical generators in series/parallel combination to meet load demand of marine vessel. In worldwide, first diesel–electric integrated propulsion system was installed in passenger liner "Queen Elizabeth II" with a four-stroke MAN L59/64 DE in 1987 [7]. These developments in marine vessels are gradually followed by tugboat system. In 1825, the first steam-driven paddle tugboat "Rufus King" was used specifically for towing ships in New York harbor [8]. Later, the development in tugboat became predominant during the period of World War II, due to their competence in deployment of troops and artillery pieces. In 1984, electro-motive DEs were introduced in tugboat propulsion system with 710 series two-stroke DE. In 2008, "Carolyn Dorothy" the first tugboat to feature diesel–electric hybrid propulsion system was manufactured by Foss Maritime Shipyard, Oregon [9].

In India, diesel–mechanical tugboats with gearbox arrangements are still in practice for driving propeller. However, standardizing and electrification of tugboats in accordance with

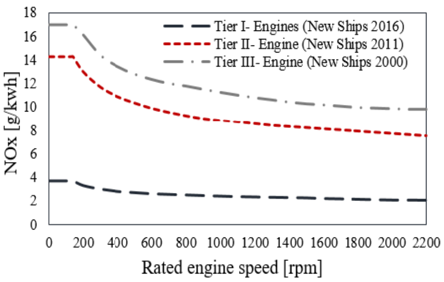

Fig. 1. Emission control limit by IMO [10].

the requirements of Indian harbors are under research. It is noted that harbor managements across the continents planned for retrofitting conventional tugboats to diesel–electric/all-electric propulsion to satisfy the emission norms imposed by international maritime organization (IMO) which is shown in Fig. 1 [10]. The primary task in any electric/hybrid vehicle is to determine installed capacity of power sources for better utilization. Hence, the key players in marine vessels and tugboats are prime movers and electric generators. The diesel electric generator for marine vessels and tugboat systems are designed as per the standards specifications defined by IEEE Std 45, IEC Publication 92 and American Bureau of Shipping (ABS) [11], [12]. In a practical scenario, electrical generators employed in marine vessels and tugboats are designed with the same type of construction and power rating for ease of exchangeability under faulty conditions [13]. Apart from that, recent developments in energy storage solutions such as battery, supercapacitor, and fuel cell had gently shifted the interest of researchers toward smart grid and dc microgrid technologies for marine applications [16]. However, the prevailing power distribution is based on ac since development of electricity and has been depicted as better choice for power transmission and distribution [17]. Therefore, till date, most practical ocean-going ships and tugboats are confined to fundamental ac distribution network in perspective of weight, space requirements, and reliability and maintenance [9], [18], [19]. Calfo *et al.* [20] illustrated numerous electrical generator configurations for marine applications.

It is important to note that fixed speed DEG employing synchronous machines (SMs) are adopted for on-board power generation in tugboat applications. It has limitation at partial generation operation, which includes wet-stacking and reduced efficiency [21], [22]. According to the manufacturers, fixed speed DEG employed for tugboat applications should be operated at a load factor of 70%–90% for better use of fuel efficiency [22], [23]. Because of these practical constraints, multiple small-capacity fixed speed DEG (operating above 60% rated capacity) are selected for tugboats in order to maintain generator load factor. Skjong *et al.* [22] analyzed the feasibility of employing multiple small-capacity power sources in marine vessels. However, utilization of multiple generators with single DE (prime mover) results in higher control complexity and uneven load sharing, which led to affect the drive cycle performance of tugboat system [21]. In order to overcome these practical limitations, each power generating unit employed in tugboat system must be coupled with separate DE, and supplementary reserves must be adopted to compensate sudden load change transients [22], [24], [25]. For effective operation of tugboat system, onboard energy management strategy (EMS) must be adopted to utilize multiple power sources and energy storage systems (ESSs) [26], [27]. In general, EMS is adopted in distributed grid-connected system, islanded system, and hybrid vehicles for controlling and monitoring the deployed multiple energy resources in order to minimize system operating cost [28]. From the literature, it has been identified that various EMS are currently in practice for different applications [27]. Particularly in the electrical vehicular technology, EMS strategy such as fuzzy logic control, deterministic based, artificial neural network, dynamic programming, and linear programming are implemented by eminent researchers [29]–[33]. Lately, prediction-based EMS for electric vehicles has gained much attention due to its better performance under dynamic constraints [34]. However, it suffers with major drawbacks such as high complex algorithms, more computation time, and need of adjustment in numerous parameters. Vu *et al*. [14] discussed an optimized EMS strategy for electric tugboat system, which results 9.31% improvement in DE fuel efficiency for electromechanical marine vessels with battery storage system. The optimization algorithm proposed in [14] schedules the power sources for every 2-min duration, and hence, the generators operating in light load region undergo frequent switching which is not practically recommended.

Several researchers in academia and industry have addressed EMS for fixed speed and variable speed generator sets with various optimal control schemes such as model predictive control, linear and nonlinear programming algorithms for marine electrical system architecture [22], [35]–[38]. However, EMS in electric tugboats by considering practical constraints (e.g., frequent start/stop) has not yet been discussed in any of the IEEE literature. It shall be noted that many researchers detailed the variable-speed operation in marine propulsion architecture, but variable-speed operation in power generating units are not yet addressed for tugboat and marine applications. This paper presents a simple optimization technique for scheduling available power sources by considering different power generators (fixed speed and variable speed) to optimally accommodate tugboat load. Furthermore, by learning the benefits of variable speed technology, a control architecture suitable for tugboat operation is proposed, in consideration of practical issues.

A. Problem Description and Importance of Presented Work

To frame simple optimization technique, a real-time tugboat load profile from ABB Singapore is adopted for scheduling available power sources and it is shown in Fig. 2 [14], [39]. From the tugboat load profile, it is observed that around 64% of total time period per driving cycle (110 min) utilizes only from 10% to 15% of installed generating capacity in loitering and waiting modes, while operating in assist low mode 50% of installed generating capacity is utilized for 20% of total time period per driving cycle, and in assist high mode 90% of installed generating capacity is utilized for 15% of the total time period per driving cycle, respectively. These operational

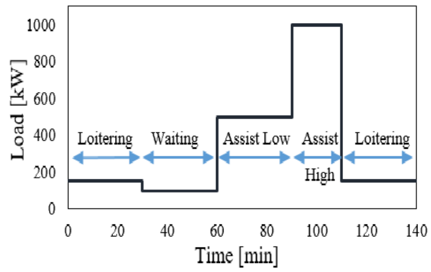

Fig. 2. Load profile of a typical tugboat [14].

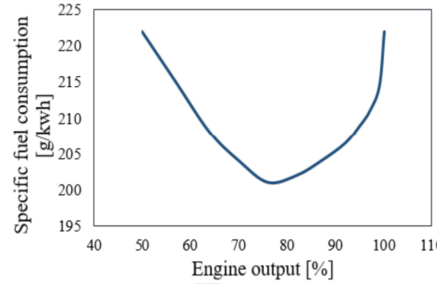

Fig. 3. SFC curve of a typical 550-kW fixed speed DE [15].

characteristics lead to drop in efficiency, in case of fixed speed DEG at part load operation (e.g., assist low mode). To overcome these operational characteristics, three prominent solutions are preferred in industry such as: 1) single fixed speed DEG employed with full-scale power converter; 2) adopting multiple fixed speed DEG sets with reduced power rating [9]; and 3) single variable-speed DE employed with doubly fed induction generator (DFIG) [40], [41]. Furthermore, it is observed that tugboat requires maximum of ±30% variable-speed operation. To enable this limited speed variation, the deployment of full-scale power converter with single fixed speed DEG increases overall system size and maintenance cost. On the other hand, solution such as multiple fixed speed DEG sets with reduced power rating and single variable-speed DE employed with DFIG are increasingly being preferred in electric power generation applications. Based on this, generalized EMS is proposed to examine fuel consumption of generating units currently in the research such as: 1) fixed speed generation (two fixed speed DE employing synchronous generators) and 2) variable speed generation (one variable speed DE employing DFIG), as shown in Fig. 4.

B. Organization of This Paper

This paper is structured as follows. The formulation of objective function to achieve minimum fuel consumption is detailed in Section II. DEG modeling and its dynamic restriction are discussed in Section III. The developed objective function for fixed speed and variable speed generating units is examined with respect to the fuel economic benefits in Section IV. Section V presents the detailed control strategy of variable speed DFIG standalone system for electric tugboat applications. Section VI discusses the simulation and experimental results to demonstrate the effectiveness of the proposed control strategy. Section VII describes the concluding remarks of the proposed variable speed generating system.

II. Optimization for Minimum Fuel Consumption

The objective function for tugboat system is formulated in consideration with specific fuel consumption (SFC) curve of fixed speed and variable speed DEG systems in order to minimize its fuel consumption. Constraints for objective function have been framed in accordance with the practical limitations of electric and mechanical equipments. For ease of calculation, some assumptions have been made such as: efficiency of batteries and generators is assumed to be 90% and 80%, respectively, when it is optimally loaded, while computing optimization algorithm, switching transients introduced by the engine, battery, and switchgears are neglected. In addition, mechanical dynamics associated with the DEG take less than 10 s to deliver rated power from its OFF state [42], [43].

For optimization, a nonlinear cost function "J_k" is developed to minimize the tugboat fuel consumption

$$\text{Min} \sum_{k=1}^{N} (J_k). \tag{1}$$

To accomplish the objective, the cost function is split into three subfunctions and is represented in the following equation:

$$J_k = \sum_{k=1}^{N} (\text{TFC}_k + \text{BP}_k + \text{PT}_K) \tag{2}$$

where TFC is the total fuel consumption, BP is the battery power, and PT is the power tracking at time index k. The terms of the cost function "J_k" are explained as follows.

A. Total Fuel Consumption

Objective of this subfunction is to minimize the SFC of DE. The TFC per driving cycle is expressed as

$$\text{TFC}_k = \sum_{k=1}^{N} \left(F_k^{\mathfrak{f},v} \times \frac{\Delta t}{(H \times d)} \right) \tag{3}$$

where F denotes the SFC curve equation, the terms $\mathfrak{f}$ and v represent the fixed speed DEG, and variable speed DEG operation at time instant k. H is the calorific value of DE oil and d is the DE oil density for time duration Δt.

Based on fixed speed SFC curve (Fig. 3), the term F is represented as quadratic function of engine output. The parameters a^s, b^s, and c^s are derived from the SFC curve of fixed speed DE [44]. E^p and E^{pr} are output power and rated power of generator, respectively, and n is number of onboard fixed speed generators. Y represents the operation status of power sources, where "1" represents ON, while "0" represents OFF

$$F_k^{\mathfrak{f}} = \sum_{k=1}^{N} \sum_{i=1}^{n} \left[\left[a_i^s \left(\frac{E_{k,i}^p}{E_i^{p_r}} \right)^2 + b_i^s \frac{E_{k,i}^p}{E_i^{p_r}} + c_i^s \right] Y_{k,i} E_{k,i}^p \times H \right]. \tag{4}$$

Similarly, a 1.1-MW variable speed SFC curve depicted in Fig. 5 is used to represent the term (F) for variable speed DEG in consideration of engine output power and

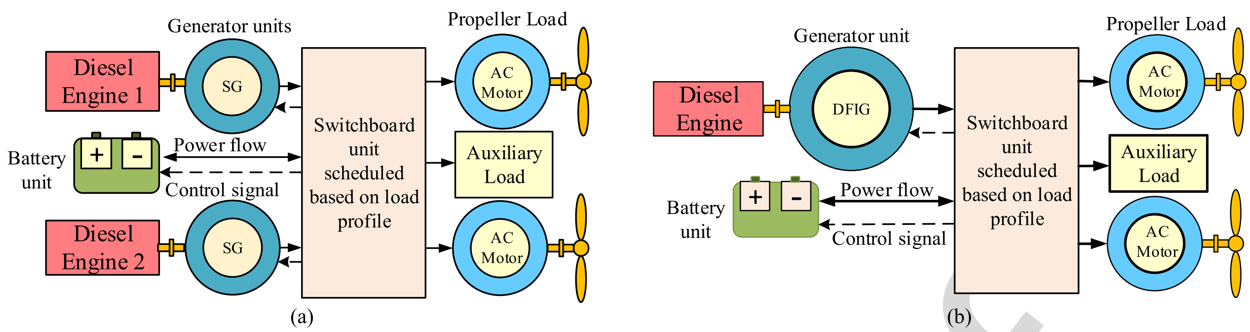

Fig. 4. Electric tugboat systems considered for this research. (a) Fixed speed DEG system. (b) Variable speed DEG system.

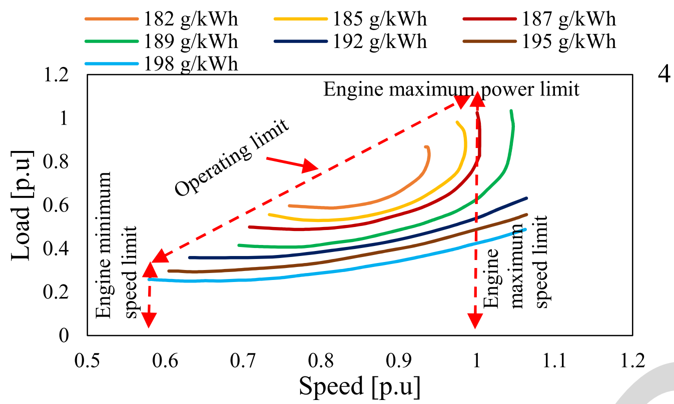

Fig. 5. SFC curve of a typical 1.1-MW variable speed DE.

operating speed [45]. The speed variability in DE is achieved by controlling fuel flowthrough actuator [46]

$$
\begin{aligned}
F_k^v &= \sum_{k=1}^{N}\left[\left[\left(\frac{E_k^d}{E^{dr}}\right)^2\left(a_1\frac{E_k^d}{E^{dr}}+a_2\frac{S_k^d}{S^{dr}}+a_3\right)+\left(\frac{S_k^d}{S^{dr}}\right)^2\right.\right.\\
&\qquad\times\left(b_1\frac{S_k^d}{S^{dr}}+b_2\frac{E_k^d}{E^{dr}}+b_3\right)+\frac{E_k^d}{E^{dr}}\left(c_1\frac{S_k^d}{S^{dr}}+c_2\right)\\
&\qquad\left.\left.+d_1\frac{S_k^d}{S^{dr}}+e_1\right]Y_k S_k^d E_k^d H\right] \qquad (5)
\end{aligned}
$$

where a_1, a_2, a_3, b_1, b_2, b_3, b_1, c_2, d_1, and e_1 are the constants related to fuel consumption with respect to speed and output power computed from curve fitting. E^d and E^{dr} are output power and rated power of variable speed DEG. S^d, and S^{dr} are the operating speed and rated speed of variable speed DEG.

From Fig. 5, it is observed that, while operating DE at 0.4-p.u. load, the fuel consumption can be reduced from 198 to 189 g/kWh by opting a variable speed technology. It consumes 91.08, 92.53, 93.97, and 95.42 L of fuel per hour at 0.74, 0.83, 0.9, and 0.98 p.u. of DE speed, respectively, when the specific gravity of diesel oil is taken as 0.83 kg/L.

B. Battery Power

The BP is represented as

$$
\mathrm{BP}_k = \sum_{k=1}^{\mathrm{N}} \bar{\Upsilon}_k E_k^{\mathrm{B}}. \qquad (6)
$$

It is initially assumed that the battery is fully charged, i.e., $\mathrm{SOC}(0) = \mathrm{SOC}^{\max}$. Also, it is mandatory to maintain the battery state of charge (SOC) in boundaries by proper charging/discharging cycle. The relationship between the SOC and BP is given as

$$
\mathrm{SOC} = \begin{cases} E(0) + \left(\dfrac{E^{\mathrm{B}}\eta_{\mathrm{ch}}\Delta t}{E^{\mathrm{cap}}}100\right), & \text{for charging} \\ E(0) - \left(\dfrac{E^{\mathrm{B}}\eta_{\mathrm{dc}}\Delta t}{E^{\mathrm{cap}}}100\right), & \text{for discharging} \end{cases} \qquad (7)
$$

where $E(0)$ represents the initial energy level of battery (SOC in %), E^{cap} is the total capacity of battery, E^{B} represent power supplied by the battery, η_{ch} and η_{dc} are the charging and discharging efficiency, and Δt is the charging/discharging time interval. The batteries may be charged with the grid supply at harbor or by DEG generated power. To identify whether batteries are charged with grid power or DEG a digital constant $\bar{\Upsilon}$ is utilized. Where $\bar{\Upsilon} = 0$ batteries are charged with grid power, and when $\bar{\Upsilon} = 1$ batteries are charged with onboard DEG. Furthermore, battery should be able to provide excitation startup power for a generating unit, once switchboard unit gives command to DEG.

C. Power Tracking

The developed subfunction tracks the load demand to minimize the surplus power during tugboat operation based on the following equation:

$$
\mathrm{PT}_k = \sum_{k=1}^{N}\sum_{i=1}^{n}\left(E_k^L - \left(E_{k,i}^p + E_k^d + E_k^B\right)\right) \cong 0 \qquad (8)
$$

where E^{L} and E^{B} are the load demand and BP supplied at time instant k.

D. Constraints

There are four sets of constraints that are considered in this optimization problem.

1) Engine Limits: The operating range of both fixed speed and variable speed DEG are limited to maximum and minimum permissible values in consideration of fuel economy and the life span of equipment

$$
E^{p\min} \le E_k^p \le E^{p\max} \qquad (9)
$$

$$
E^{d\min} \le E_k^d \le E^{d\max} \qquad (10)
$$

$$
-Rd_i\Delta t \le E_{k,i}^p - E_{k-1,i}^p \le Ru_i\Delta t \qquad (11)
$$

where $E^{p\min}$, $E^{p\max}$, $E^{d\min}$, and $E^{d\max}$ are the minimum and maximum allowable output power for fixed speed and variable speed DEG, respectively. Ru_i and Rd_i represent the ith generator ramp-up and ramp-down rate, respectively. Generally, there is some reserve capacity (spinning reserve) backed by power sources to deal with sudden changes in load. Hence, the capacity of generators is chosen above the load demand in order to meet sudden transient in load current.

2) Battery Limits: The charging and discharging limits of battery and SOC limits are represented as

$$-E^{\mathrm{Ch.max}} \le E_k^{\mathrm{B}} \le E^{\mathrm{DCh.max}} \tag{12}$$

$$\mathrm{SOC}^{\min} \le \mathrm{SOC}_k \le \mathrm{SOC}^{\max} \tag{13}$$

where $E^{\mathrm{Ch.\ max}}$ and $E^{\mathrm{DCh.max}}$ are the charging and discharging limits of battery, $\mathrm{SOC}^{\min}$ and $\mathrm{SOC}^{\max}$ are the minimum and maximum SOC of battery.

3) Load Demand Response: At any instant of time, cumulative power generated via power sources should meet the net load demand. This constraint is mathematically represented as follows:

$$E_k^p + E_k^d + E_k^{\mathrm{B}} \ge E_k^{\mathrm{L}}. \tag{14}$$

In general, loading/unloading of tugboat system is performed gradually. However, the pulsating loads in tugboat systems are accommodated by fast responding ESS.

4) Variable Speed Limit: The speed variation of DFIG should be limited in consideration with the slip power requirements

$$S^{d\min} \le S^d \le S^{d\max}. \tag{15}$$

Hence, the formulated optimization problem, minimize cost function "J" given in (2) subject to constraints from (9) to (15). Performance-related parameters such as power generated by each generator, fuel consumption, and battery status with respect to time are detailed in Section IV.

III. Diesel Engine Generator Modeling

As aforementioned, DEG is the key player in tugboats. The mechanical torque produced by internal combustion in DE is the accumulation of torques from each cylinder. Typically, multicylinder DE operates with certain firing imbalance giving rise to pressure difference in cylinders. In general, the permissible pressure difference is 0.5 bar. The excess pressure difference and misfiring of cylinders cause uneven power distribution on crankshaft, which results fluctuation in mechanical torque output. In practical operation, DEG load is varied smoothly, and sudden change in load is restricted due to its sluggish dynamic nature. The foremost reason for the response delay in DE is ignition delay and power stroke delay during DE fuel combustion. Ignition delay represents the time required by fuel–air mixture for complete combustion and time required by each cylinder to respond load variation is termed as power stoke delay [47]. This dynamic behavior of DE coupled with electric generator results power quality issues during startup and sudden load change. In tugboats, sudden load demand is required for dynamic positioning,

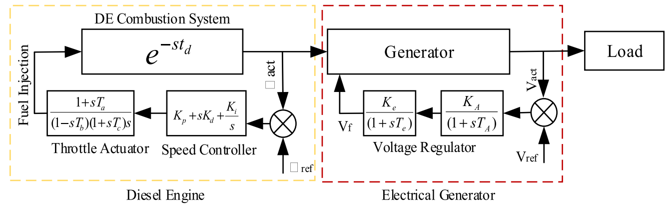

Fig. 6. DE generator model.

wave compensators, and critical load operation. The sudden load rise causes abrupt disturbances in busbar frequency. To avoid system failure under frequency dip, a practical operation procedure is to rapidly reduce noncritical loads. Once noncritical load is reduced to its set point value, then DE load is increased slowly to maintain bus-bar frequency within tolerance limit. BØ examined multiple fixed speed AQ:5 DEG system under various dynamic behavior conditions and concluded that when load is varied smoothly from 5% to 75% of its installed capacity in 25 s the system frequency is within the acceptable level. If the same amount of load is varied in 2.5 s the system frequency violates the safety tolerance limit [48]. Moreover, the author proposed that the system frequency can be maintained under fast varying load by effectively controlling the DE fuel rate. In case of variable speed DEG, the system frequency is maintained constant under dynamic operating conditions through the power electronic converters. To meet the power delivery, during the delay caused in DEG starting, supplementary reserves (supercapacitors, battery units, fuel cells, and flywheel) are used [49], [50].

Before performing optimization on test system, dynamic behavior of DEG is studied through mathematical models of speed controller, throttle actuator, and engine delay unit in MATLAB Simulink environment. The mathematical model of DE speed control is modeled, as shown in Fig. 6. The modeling procedure and controller parameters estimation are addressed in [51]–[53]. In this paper, the parameters of KTAA19-G6A model, four stroke, six cylinders, 1500 r/min, and 550-kW DE manufactured by CCEC Cummins [54] is used to design fixed speed DEG. For variable speed DEG, LF-1200GF model, four stroke, 12 cylinders, 1500 r/min, and 1.1-MW DEG manufactured by Lovol is used [55]. The reference speed for fixed speed DE is determined by the desired generator frequency. For variable-speed operation, DE speed reference is provided through a lookup table. The input parameters to the lookup table are load demand and operating speed. In order to minimize the SFC, the optimal DE speed is estimated from the load versus speed profile, as shown in Fig. 5. The parameters of PID controllers, time constants of throttle actuator, and voltage regulator are given in Appendix A (control parameters). The time delay t_d of DE combustion is calculated by

$$t_d = \frac{30 s_t + 15n}{\omega n} \tag{16}$$

where s_t is the number of strokes, ω is the engine speed in revolution per minute, and n is the number of cylinders.

The dynamic behavior of fixed and variable speed DEG during startup is shown in Fig. 7. In Fig. 7(a) and (c), it is inferred

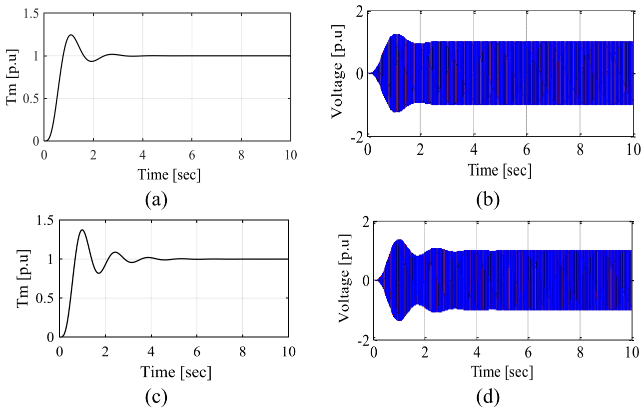

Fig. 7. DE generator simulation results. (a) 550-kW fixed speed DEG mechanical torque. (b) 550-kW fixed speed DEG terminal voltage. (c) 1.1-MW variable speed DEG mechanical torque. (d) 1.1-MW variable speed DEG terminal voltage.

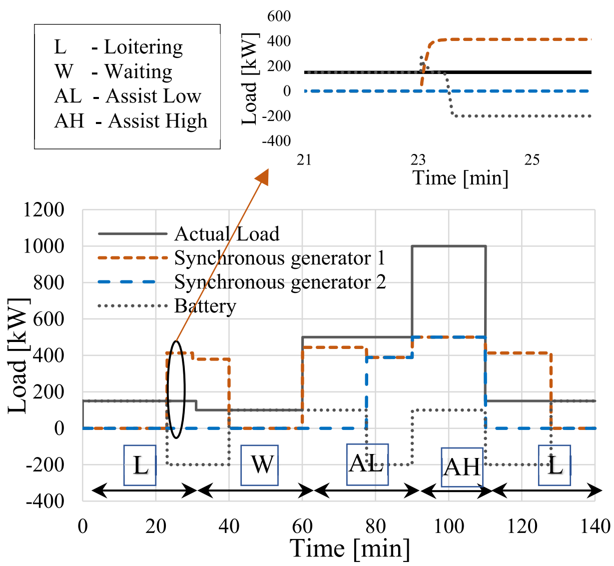

Fig. 8. Fixed speed DEG system optimal power management.

that 550-kW fixed speed DEG takes 4 s and 1.1-MW variable speed DEG takes 5.6 s to generate required mechanical torque from their ideal position. Fig. 7(b) and (d) shows the voltage buildup of 550-kW fixed speed DEG and variable speed DEG, respectively. DEG dynamic behavior during startup is shown in zoomed part in Figs. 8 and 9 for fixed and variable-speed operations. This delay in the generator is acquired by multiplying exponential delay constant "Đ" resembling the delay caused due to the sluggish dynamics of the DE with the output generated power "$E^p_{k,i}$"variable obtained through optimization

$$Đ = \left(1 - e^{\frac{-t}{\tau}}\right) \tag{17}$$

where τ is the time delay taken by DEG to generate rated power from its initial state of rest. In this analysis, time delay constant τ is taken as 0.07 for fixed speed DEG. However, the variable speed DEG takes longer time to reach its rated

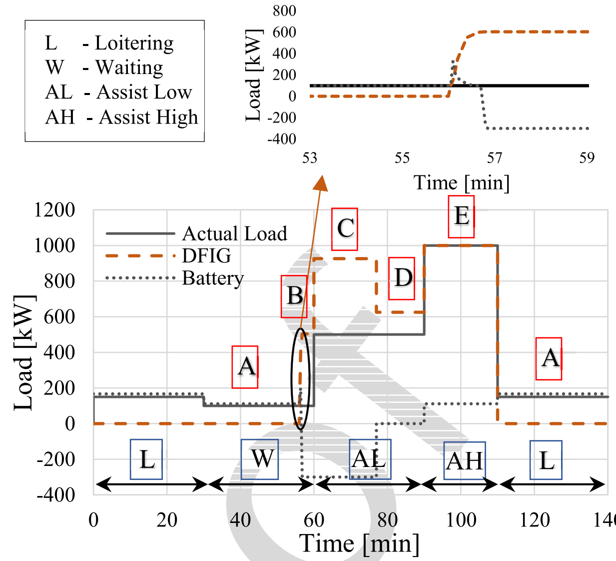

Fig. 9. Variable speed DEG system optimal power management.

speed when compared with fixed speed DEG. For variable-speed operation, time delay τ is calculated as 0.09.

IV. System Parameters and Optimization Results

In case of fixed speed operation, two no's of 550-kW DEG with 100-kWh battery storage system is considered for analysis. The set limits for battery SOC maxima and minima are chosen as 90% and 20%, respectively. Furthermore, during the computational process DE efficiency and electrical generator efficiency are considered as 80%. The detailed parameters and optimization constraints are shown in Appendix A (optimization parameters). In case of variable-speed operation, a single 1.1-MW DFIG unit with 200-kWh battery storage system is considered for analysis. The battery storage system is adopted in accordance with slip variation of ± 0.3 p.u. The nonlinear equation formulated in Section II is minimized using the fmincon function, a local optimizer that uses sequential quadratic programming subject to linear and nonlinear constraints. For plotting optimal energy management curves optimization toolbox in MATLAB is used.

A. Case 1: Fixed Speed Generators

In fixed speed operation, two no's of DEG are responsible for maintaining system voltage and frequency. If two generators are in operating conditions, tugboat must share the load equally among the generators for safety concern of DEG units [56]. The cost function derived for fixed speed DEG is represented in

$$J = \sum_{k=1}^{N} \sum_{i=1}^{n} \left[\left[\left[a_i^s \left(\frac{E^p_{k,i}}{E_i^{Pr}} \right)^2 + b_i^s \frac{E^p_{k,i}}{E_i^{Pr}} + c_i^s \right] Y_{k,i} E^p_{k,i} \times H \right.\right.$$
$$\left.\left. + \alpha \left(E_k^{\mathrm{L}} - \left(E^p_{k,i} + E_k^{\mathrm{B}} \right) \right) \right] + \beta \bar{\Upsilon}_k E_k^{\mathrm{B}} \right] \times \frac{\Delta t}{(H \times d)} \tag{18}$$

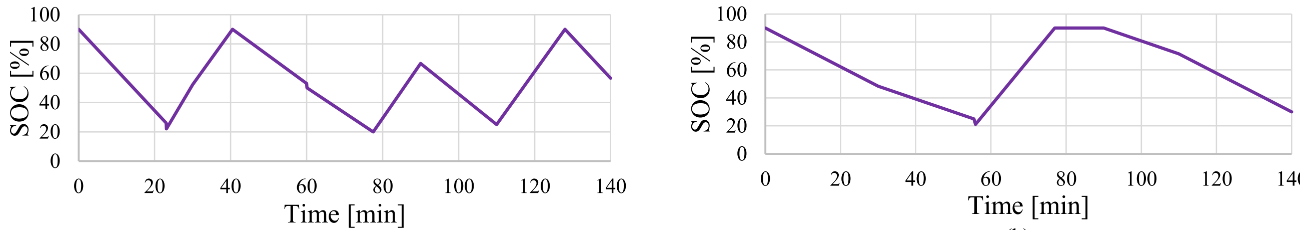

(a) (b)

Fig. 10. SOC of battery. (a) Fixed speed DEG system. (b) Variable speed DEG system.

TABLE I
FUEL CONSUMPTION

Tugboat system	Proposed methodology fuel consumption (per cycle)	Fuel saving (%)	Co₂ emission (kg)	Revenue saved ($/yr)	Rule-base fuel consumption (per cycle)
Mechanical DE propelled system	241.6 L	--	641.3	--	--
Fixed speed DEG system (without battery)	214 L	11.42 %	568.1	29,617.6	233 L
Fixed speed DEG system (case 1)	174.43 L	27.8 %	463	72,080.2	188.9 L
Variable speed DEG system (case 2)	169.44 L	29.86 %	450.3	77,434.9	183.1 L

$$J = \sum_{k=0}^{\mathrm{N}} \Bigg[\Bigg[\left(\frac{E_k^d}{E^{dr}}\right)^2 \left(a_1 \frac{E_k^d}{E^{dr}} + a_2 \frac{S_k^d}{S^{dr}} + a_3\right) + \left(\frac{S_k^d}{S^{dr}}\right)^2 \times \left(b_1 \frac{S_k^d}{S^{dr}} + b_2 \frac{E_k^d}{E^{dr}} + b_3\right) + \frac{E_k^d}{E^{dr}} \left(c_1 \frac{S_k^d}{S^{dr}} + c_2\right) + d_1 \frac{S_k^d}{S^{dr}} e_1 \Bigg] S_k^d E_k^d H + \alpha\left(E_k^{\mathrm{L}} - \left(E_k^d + E_k^{\mathrm{B}}\right)\right) + \beta \bar{\Upsilon}_k E_k^{\mathrm{B}} \Bigg] \times \frac{\Delta t}{(H \times d)}. \tag{19}$$

The penalty weights α and β are selected such that fuel consumption parameters dominate the other terms in cost function. The optimization results and SOC of the battery are shown in Figs. 8 and 10(a)

From the results, it is observed that less number of switchover occurred in DEG throughout the load drive cycle in comparison with results reported in [14], which is an additional advantage of this paper in view of practical implementation. The optimization algorithm determines the operational strategy for generators and batteries in order to meet tugboat load profile. It shall be noted that batteries accommodate light loads, whereas higher loads are shared by fixed speed DEG sets at their highest possible efficiency. In addition, the algorithm enforces battery to maintain the required SOC limits to increase its life span.

B. Case 2: Single Variable Speed Generator

In variable-speed operation, rotor excitation circuit employed in DFIG maintains the system frequency. The cost function derived for variable-speed operation is represented in (19). The obtained optimization result is shown in Fig. 9, and SOC of battery is shown in Fig. 10(b). In Fig. 9, power generation variation in variable speed DEG is denoted by segments "A–E." At segment "A" variable speed DEG is at idle mode and in segment "B–E" DFIG operate in stator frequency regulation mode to meet the load demented by the tugboat.

C. Fuel Economic Analysis for DEG System

The fuel consumption for fixed speed and variable speed 1.1-MW DEG system operated for 7 h/day (three cycles/day) is considered for economic analysis and results are tabulated in Table I. The variable speed DEG system is compared with conventional mechanical DE propelled system and fixed speed DEG system (2×550 kW with battery). From the analysis, it is observed that variable speed DEG consumes 29.86% less fuel in comparison with conventional mechanical DE propelled system and 2.9% less fuel in comparison with fixed speed DEG system (2×550 kW with battery). Furthermore, it is noted that 29.8% of CO_2 emission is reduced by adopting variable speed DEG system with the revenue saving of 77434.9 $/year in consideration of fuel cost at 0.98 $/L.

The optimization strategy adopted in this paper is also compared with conventional rule base EMS in Table I [57], [58]. The rule base EMS working rules are as follows.

1) Battery SOC is maintained within tolerance limits.
2) If the SOC reaches to its minimum threshold value, the battery is charged using available DEGs.
3) At light-loads the battery is used to meet load demand.
4) At high-loads DEG should be used to meet the load demand. From Table I, it is observed that the proposed algorithm offers an overall improvement of 8% in comparison with conventional rule-based EMS.

D. Uncertainty Analysis

Generally, in any optimization process unknown parameters are randomly chosen from search space and updated iteratively with best suited value to have a convergence in optimal solution. While estimating unknown parameters there may be uncertainty, which diverge optimal solution. There are several

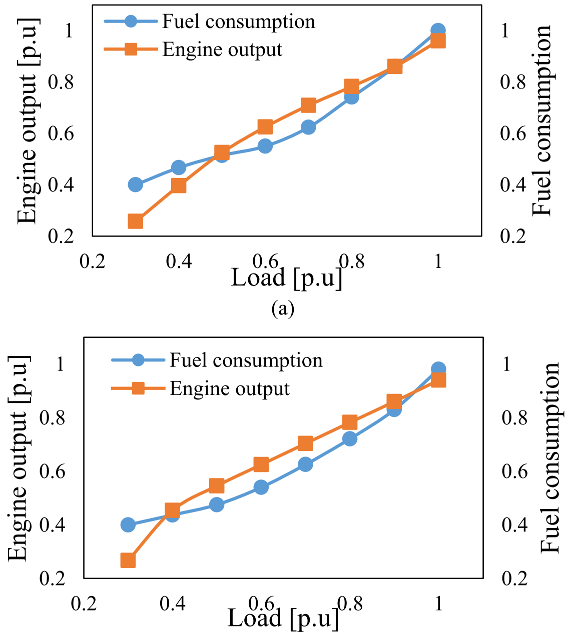

Fig. 11. Uncertainty analysis results. (a) Fixed speed DEG system. (b) Variable speed DEG system.

contributions on uncertainty analysis to identify parameter change [59], [60]. Sensitivity analysis is an effective method to quantify the impact of single input variable on the system performance. In this paper, DEG load is varied, and the effect on system fuel consumption is shown in Fig. 11(a) and (b) for fixed and variable speed DEG system. From the graph, it is illustrated that the engine output varies linearly with load. Fuel consumption (in graph) is in relation with proposed methodology fuel consumption, as it is tabulated in Table I (case 1 for fixed speed and case 2 for variable speed). The slope in fuel consumption is due to the nature of DEG system SFC curve. It is noted that the fuel consumption is minimum in region, where DEG is loaded at 70%–85% of its rated capacity. At low-load region, variable speed DEG system provides better fuel efficiency in comparison with fixed speed DEG system. The optimal region for DEG system is to operate in the intersected area of engine output and fuel consumption. Hence, the adopted algorithm is robust for optimal operation of DEG system at the load laying in intersected area. In this paper, the unknown parameters are dependent on the SFC curve and known parameters are tabulated in Appendix A. Moreover, the unknown parameters obtained from optimization algorithm are always within safety operational limits.

V. Proposed Energy Efficient Variable DEG Drive Operation

From Section IV, it is identified that variable speed DEG system had best fuel economy in comparison with the other conventional tugboat generation systems. To adopt variable speed technology in DEG system, a proper control strategy must be designed for its efficient operation. The control strategy adopted for DFIG system in standalone operation mode is shown in Fig. 12. The proposed system consists of DFIG with additional battery bank to meet load requirements of tugboat, as shown in Fig. 2. The battery bank is adopted to meet 20% of tugboat load demand at loitering and waiting modes. In addition to this battery, bank builds up initial stator flux for DFIG through machine-side converter (MSC). The optimal speed of DE is estimated in consideration of SFC curve and load demand. The proposed variable speed DEG system operates in three modes such as: 1) idle mode (less than 20% of tugboat load); 2) initial stator flux mode; and 3) stator frequency regulation mode. If generator is at idle mode, battery bank supplies power through dc–dc converter to maintain dc-link voltage at desired level. At that instant, load-side converter (LSC) acts as inverter to meet tugboat load demand (at loitering and waiting modes). Once the switching unit commands generating system, the DFIG initial stator flux requirement is fed through MSC with precharged dc link. Thereafter, real power is delivered to tugboat system through stator terminals. Furthermore, the system frequency is maintained through rotor excitation circuit in the stator frequency regulation mode.

A. Control Strategy: Idle Mode

At the idle mode, the circuit breaker B_1 is at open position, and battery bank is connected to dc link through dc–dc converter to precharge dc-link capacitance. The battery bank voltage is chosen lower than dc-link voltage to implement bidirectional operation (charging/discharging). The employed dc–dc converter operates in continuous conduction mode. Initially, DEG is kept in idle mode up to 20% of tugboat load for best fuel economy. At that instant, battery bank feed power to dc-link capacitance by switching dc–dc converter. The dc–dc converter operates in boost mode by providing high frequency gate pulse to switch S_2 for particular interval to store energy in inductor. At the instant S_2 is turned off antiparallel diode incorporated with switch S_1 starts to conduct. Meanwhile, LSC is provided with sine pulsewidth modulation (SPWM) to meet on-board load requirement of tugboat and MSC gated with dead pulse pattern.

B. Control Strategy: Initial Reactive Power Mode

In this mode, desired load torque is generated for DFIG with the operation of DE. While operating DFIG in standalone mode, it demands initial excitation to generate voltage across stator terminals. The implemented vector control algorithm regulates the machine reactive and active power flow by controlling rotor d–q axes currents. The MSC controls rotor currents in stator flux orientation frame to obtain stable operation. The initial reactive power mode is fed through MSC based on d-axis rotor current control. Once DFIG generates desired system frequency/voltage, breaker switch B_1 is properly synchronized to meet tugboat load demand. Meanwhile, switch S_1 in dc–dc converter is gated to charge battery bank. For convenient operation of this mode, 10% of battery reserve is safeguarded.

C. Control Strategy: Stator Frequency Regulation Mode

The rated stator flux and dc-link voltage are maintained by keeping the stator flux reference constant. The decoupled

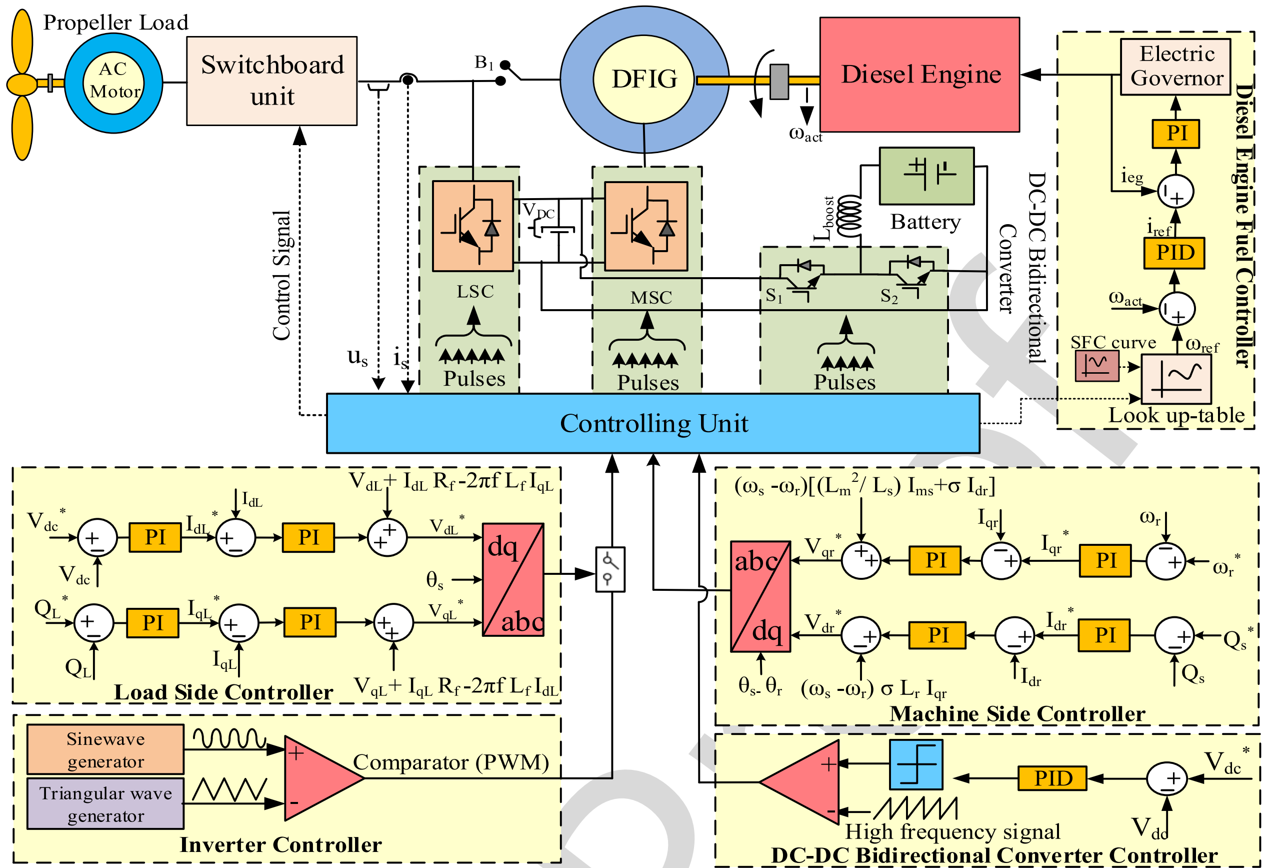

Fig. 12. Control strategy in DFIG for tugboat application.

control implemented in both the LSC and MSC ensure the control of active and reactive power of DFIG. The dc-link voltage is stabilized using LSC regardless of the magnitude and direction of the rotor voltages and currents.

The load side d-axis current component is used to regulate the dc-link voltage

$$P_{\mathrm{L}} = \frac{3}{2} V_{\mathrm{L}} I_{d\mathrm{L}}. \tag{20}$$

The load side q-axis current component used to regulate stator reactive power

$$Q_{\mathrm{L}} = -\frac{3}{2} V_{\mathrm{L}} I_{q\mathrm{L}}. \tag{21}$$

The q-axis rotor current controls the electromagnetic torque of the machine, which indirectly controls the speed and d-axis current controls the machine reactive power

$$\text{Electromagnetic torque, } T_e = -\frac{3}{2} P \left(\frac{\mathrm{L}_m^2}{\mathrm{L}_s}\right) I_{ms} I_{qr} \tag{22}$$

$$\text{Reactive power, } Q_m = \frac{3}{2} V_{\mathrm{L}} \left(\frac{\Psi_s L_m}{(\mathrm{L}_s - \mathrm{L}_m)}\right) I_{dr}. \tag{23}$$

The variation in stator frequency due to varying torque/load profile of tugboat will be regulated by both the MSC and LSC.

VI. Simulation Results and Experimental Validation

A. Simulation Results

In order to validate the effectiveness of proposed control strategy, a 1.1-MW DFIG system is simulated in MATLAB/Simulink environment with given tugboat load profile (shown in Fig. 2). The machine parameters are given in Appendix B. A 2-level back-to-back voltage source converter (2L-VSC) is connected to rotor circuit of DFIG. The switching frequency of 5 kHz is chosen for MSC to regulate the machine reactive power requirement. The dc-link voltage is maintained at 1200 V (10 000 μF) by LSC with 5-kHz switching frequency. The sampling time is selected as $1e^{-5}$ during simulation.

In simulation, battery bank is considered as a constant dc source with 800 V, and boost inductor value is selected as $L_{\mathrm{boost}} = 7.81\ \mu$H. For continuous conduction mode of operation, the dc–dc converter switching frequency is considered as 8 kHz based on 0.5% voltage ripple. To represent the voltage profile in sine wave the filter circuits are designed with cutoff frequency of 750 Hz and damping factor (ð = 0.707). In standalone DFIG system, the propeller and auxiliary loads are considered as 1-MW dynamic load. To reduce simulation computation time, 140-min tugboat driving cycle time is scaled down to 140 s. The performance of the proposed control strategy for variable speed DEG system is shown in Fig. 13. The simulation results are divided into five segments denoted

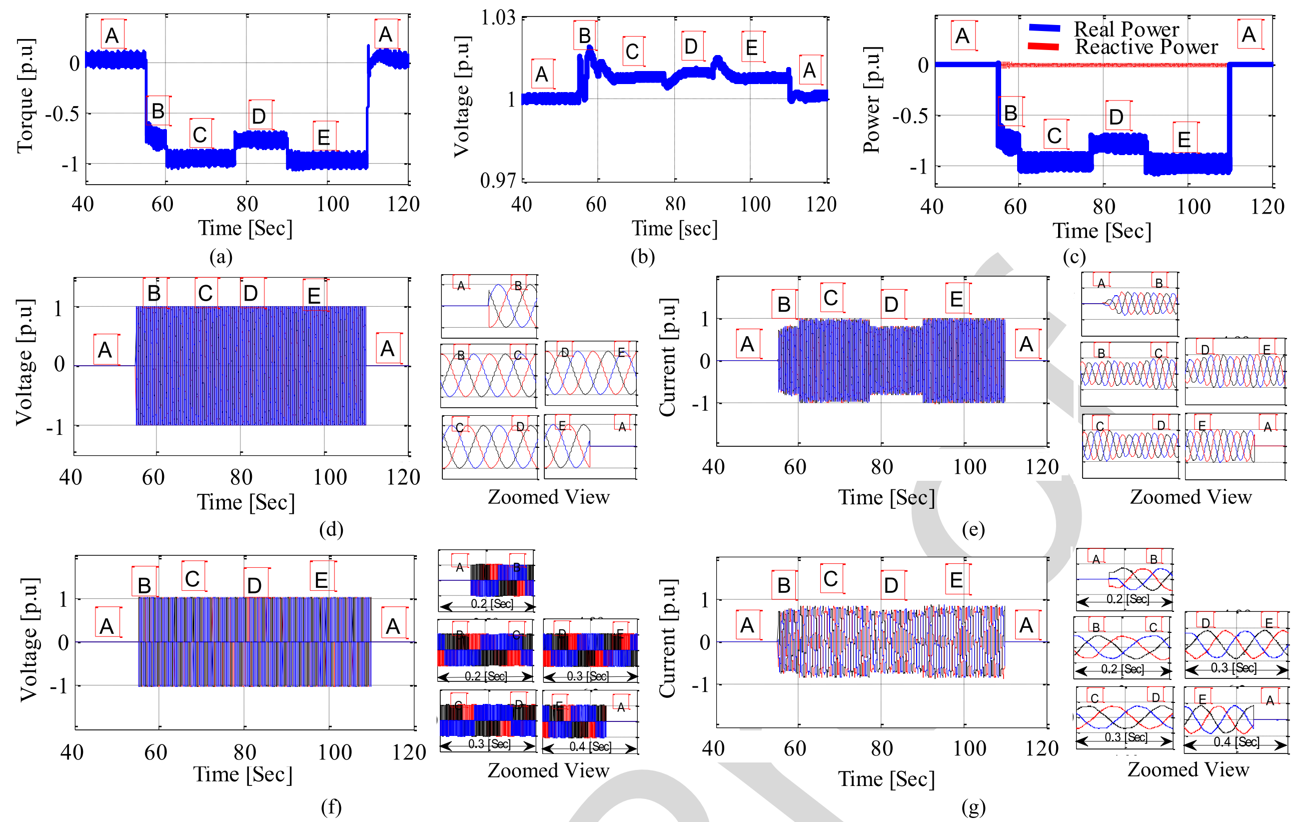

Fig. 13. Performance of proposed control strategy for variable speed DEG system. (a) Torque (p.u.). (b) DC-link voltage. (c) Real and reactive power. (d) Stator voltage. (e) Stator current. (f) Rotor voltage. (g) Rotor current.

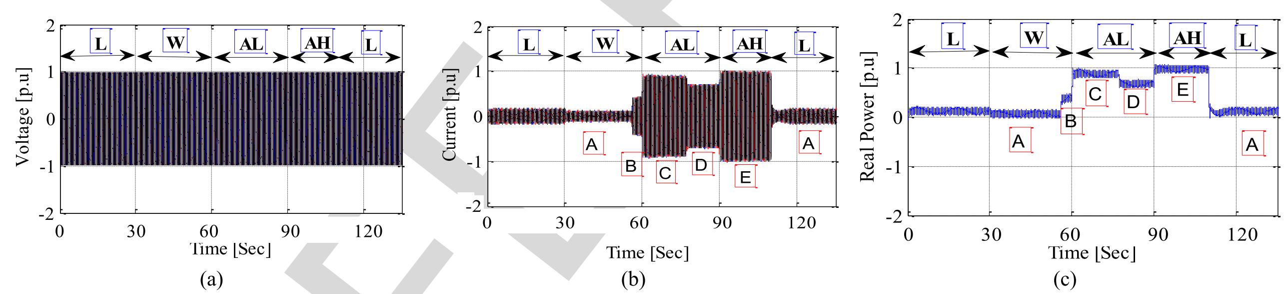

Fig. 14. Load current profile of tugboat at various loading conditions. (a) Load voltage. (b) Load current. (c) Real power consumption.

as "A–E." At "A" required power is delivered by the battery, and DFIG is at ideal operation mode (mechanical torque is zero). From Fig. 13(a), it is inferred that wide variation of mechanical torque is generated at segments "B–E" to accommodate assist low and assist high load profile. In segment "B," 0.75-p.u. mechanical torque is applied to accommodate the load. During the starting of DFIG at segment "B" acceptable transients in dc-link voltage (1.016 p.u.) are observed due to the synchronization process, as shown in Fig. 13(b). Later on, MSC controller maintains constant dc-link voltage within permissible limit of 5%. At segment "C" load changed to 0.92 p.u. from 0.5 p.u. Since the tugboat load is varied smoothly in real-time operation, a rate limiter block is designed for simulation. The real and reactive powers generated during the load change are shown in Fig. 13(c). At segment "D" reduction of mechanical torque from 0.96 to 0.7 p.u. signifies the change in applied load from 0.92 to 0.62 p.u. In high assist mode (segment "E"), the generator is instructed to meet rated torque. Fig. 13(d) and (f) shows the stator voltage and rotor voltage, respectively. From the zoomed-in view, it can be seen that stator voltage is maintained constant (1 p.u.) throughout ("B–E" segment) with the help of rotor excitation circuit. The varying tugboat load influences on the magnitude of stator and rotor current, as shown in Fig. 13(e) and (g). The stator frequency is maintained at desired level (50 Hz) through MSC, under varying mechanical torque. In order to maintain the stator frequency constant at segment "B," the rotor frequency of 10 Hz is injected through MSC, as shown in Fig. 13(g) (zoomed part). The same operational characteristic is repeated in segment "C (5 Hz), D (7 Hz), and E (2 Hz)" by MSC to deliver power at desired system frequency. Fig. 14(c) shows the real power consumption at various loads of tugboat. From Fig. 14(b), it is seen that the tugboat draws load current of 0.17 and 0.12 p.u. during loitering and waiting modes

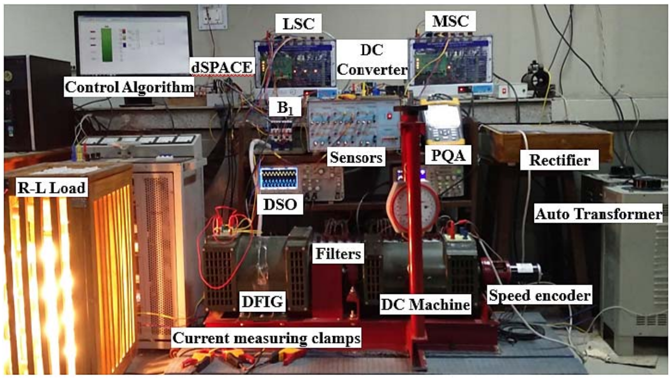

Fig. 15. Experimental setup.

of operation, while operating in waiting and assist low mode it draws about 0.51, 0.93, and 0.62 p.u. of load current (segment "B–D") and in assist high mode it draws 1 p.u. of load current (segment "E"). With respect to these load currents, fuel consumption for variable speed DEG system is computed as 169.6 L per driving cycle. As aforementioned, based on SFC curve (Fig. 3), fixed speed DEG system (2 × 550 kW) consumes about 174.43 L per driving cycle. From the computed fuel consumption, it is concluded that variable speed DEG system saves about 2.9% of fuel in comparison with fixed speed DEG system (with battery).

B. Experimental Results

To validate the effectiveness of proposed control strategy, experimentation has been performed through a 2.2-kW DFIG prototype with 2L-VSC for its rotor excitation circuit, as shown in Fig. 15. The employed 2L-VSC is constructed using SKM100GB12T4 SEMITRANS IGBT modules and is interconnected with 4700 μF/450 V common dc-link capacitors to handle slip power requirements. In addition, prototype comprises of LA 55-P Hall effect current sensor, LV 20-P voltage sensor and quadrature encoder pulse (QEP) encoder (1024 pulses per revolution) for speed and position measurements. For real-time operation, measured signals are integrated to ADC channel of dSPACE MicroLabBox (DS1202) AQ:6 real-time controller. Optocoupler is used to provide isolation between DS1202 and IGBT switches, it is incorporated with fault protection. The control algorithm is designed in MATLAB Simulink environment, is transformed to C code using Simulink coder for real-time interface. The real-time interface can be configured to hardware through Control Desk 5.1 software tool. The proposed control algorithm generates 3-kHz SPWM with dead band of 6 μs to drive both the LSC and MSC. The breaker switch B_1 (L&T MNX 32) with relay is controlled by real-time controller. In experimental validation, a separately excited dc machine (3 hp) is used as prime mover to drive DFIG. Variable speed DEG speed-load characteristics are matched by controlling the torque of dc machine. The battery bank is replaced with diode bridge rectifier to charge dc-link capacitance at starting purpose. The parameters of test machine are listed in Appendix B.

During idle mode, the dc-link capacitor is charged through diode bridge rectifier. Meanwhile, LSC is provided with

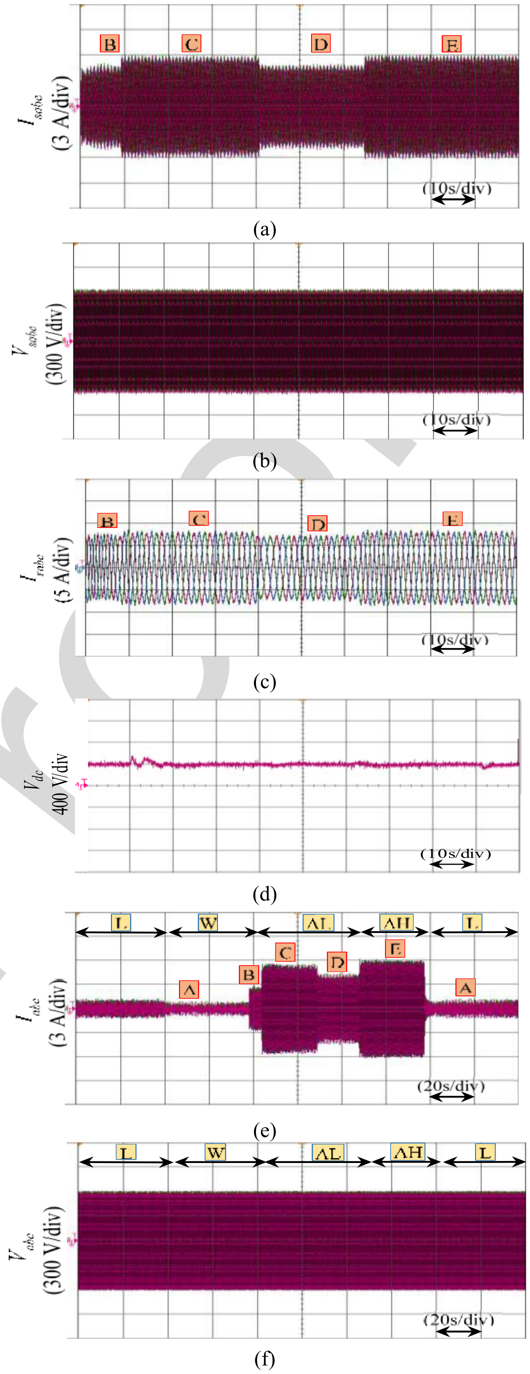

Fig. 16. Experimental validation of proposed control statergy for standalone DFIG. (a) Generator stator current. (b) Generator stator voltage. (c) Generator rotor current. (d) dc-link voltage. (e) Load curent. (f) Load volatge.

SPWM to operate in inverter mode to accommodate light loads [loitering (0.33 kW) and waiting mode (0.22 kW)], it can be observed in Fig. 16(e) denoted as segment "A." During experimentation, dc-link voltage is maintained at 375 V through diode bridge rectifier [Fig. 16(d)]. In segment "B," DFIG is rotated with the help of prime mover at 1260 r/min to accommodate 1.1 kW of load. In order to maintain the stator frequency constant (50 Hz) in segment "B" slip frequency of 8 Hz is injected through MSC, it can be observed from Fig. 16(c). From Fig. 16(d), it can be observed that small oscillations in

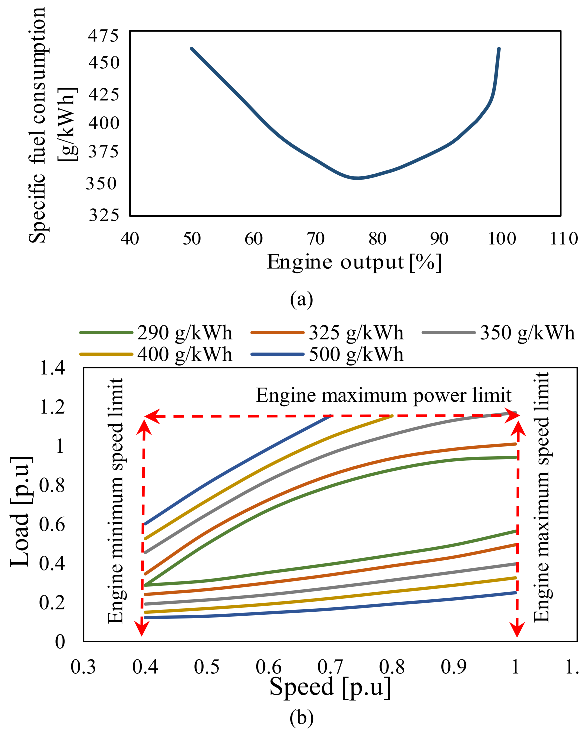

Fig. 17. SFC curve. (a) 1-kW fixed speed DE. (b) 2.2-kW variable speed DE.

dc-link voltage occur during change in load. These dc-link oscillations are settled down within short duration of time due to the effective performance of vector control strategy, while operating in assist low mode in segments "C–D" prime mover is rotated at 1350 r/min ("C") and 1290 r/min ("D") to accommodate loads of 2 kW ("C") and 1.3 kW ("D"), respectively. To deliver desired load frequency, MSC injects slip frequency of 5 Hz ("C") and 7 Hz ("D"), it can be seen in Fig. 16(c). In assist high mode, prime mover is rotated at 1440 r/min ("E") with rotor slip frequency of 2 Hz to deliver rated power of 2.2 kW. It shall be noted that in experimentation prime mover speed variation is done manually by varying field rheostat of dc machine. On the other hand, fast responding vector control strategy maintains the desired voltage/frequency of system under varying speed. Fig. 16(a) and (c) shows stator and rotor current waveforms, respectively. The stator and load voltages are maintained constant at 415 V throughout the experiment [Fig. 16(b) and (f)]. Fig. 16(e) shows the load current profile of tugboat during various operating conditions.

C. Estimated Experimental Fuel Consumption

For estimating experimental fuel consumption for fixed speed DEG system, two no's of 1.1-kW fixed speed DEG employing SM are considered. Fig. 17(a) shows the typical fuel consumption curve of a 1.1-kW fixed speed DE. The tugboat load profile is scaled down to 2.2 kW, and the battery pack is assumed to be capacity of 0.5 kWh. As represented in experimental setup a 2.2-kW DFIG is considered as proposed variable speed DE system. Fig. 17(b) shows the typical fuel consumption curve of a 2.2-kW variable speed DE. From Figs. 13(e) and 16(a), it is observed that the experimental load current profile is similar to the simulation results obtained. From Fig. 16(e), it is estimated that variable speed DEG employing DFIG unit consumes about 2.04 L per driving cycle. However, the DEG employing SM consumes 2.1 L per driving cycle, calculated based on SFC curve [Fig. 17(a)]. From the results, it is estimated that the variable speed DEG unit saves about 2.85% of fuel per driving cycle which validates the simulation results.

VII. Conclusion

In this paper, optimal energy management for diesel–electric tugboat aiming at minimum operation cost, GHG emissions reduction, considering possible technical and operational constraints is presented. In order to achieve the optimization goal, tugboat is powered from a best suited combination of fixed speed generator/variable speed generator and battery to meet the onboard power demand. Furthermore, economic analysis for both the fixed speed and variable DEG system is considered. From the analysis, it is observed that single variable-speed DEG driven tugboat offered 29.86% fuel saving in comparison with conventional mechanical DE propelled tugboat serving in Indian harbor. Similarly, the proposed variable speed DEG system (case 2) provides 2.9% fuel saving in comparison with fixed speed DEG system (case 1). For efficient operation of proposed variable speed system, a suitable control strategy is designed. The obtained simulation results confirm the viability of proposed methodology for tugboat operation. Practical compatibility of proposed variable speed DEG system was validated through a 2.2-kW DFIG experimental setup. The proposed system successfully offers less fuel consumption per driving cycle and hence reduction in operating cost and CO_2 emission.

Appendix

A. Optimization Parameters

The optimization parameters are listed in the following table.

		Case (i)			
E_i^{pr}	550 kW	E^{cap}	100 kWh	$E^{p_{max}}$	550 kW
$E^{p_{min}}$	220 kW	$E^{Ch.max}$	200 kW	$E^{DCh.max}$	200 kW
SOC^{min}	20%	SOC^{max}	90%	Rd_i	275 kW
Ru_i	275 kW	η_{ch}	0.9	η_{dh}	0.9
		Case (ii)			
E^{dr}	1.1 MW	$E^{d_{max}}$	1.1 MW	$E^{d_{min}}$	400 kW
E^{cap}	200 kWh	$E^{Ch.max}$	400 kW	$E^{DCh.max}$	400 kW
SOC^{max}	90%	SOC^{min}	20%	$S^{d_{max}}$	1 p.u
$S^{d_{min}}$	0.7 p.u	Rd_i	600 kW	Ru_i	600 kW
		Fuel consumption constants			
a^s	$30.12*10^{-3}$	b^s	-4.668	c^s	616.3
a_1	570.3	a_2	-229.1	a_3	293.1
b_1	60.71	b_2	136.1	b_3	42.47
c_1	-382.5	c_2	-686.4	d_1	213.1
e_1	288.3	H	43.2 MJ/kg	d	0.83 kg/L
		Control parameters			
T_a	0.01	T_b	0.02	T_c	0.05
K_p	0.2	K_i	0.038	K_d	0.019
K_e	1	T_e	0.73	K_A	1
T_A	1.01				

B. Parameters of Test Machine

The parameters of test machine are listed in the following table.

1.1 MW DFIG			
Power	1.1 MW	Stator resistance	2.65 mΩ
Stator Voltage	690 volts	Stator inductance	0.1687 mH
Rotor resistance	2.63 mΩ	Rotor inductance	0.1337 mH
Stator Current	1100 amps	Magnetizing inductance	5.48 mH
Frequency	50 Hz		
2.2 kW DFIG			
Power	2.2 kW	Stator resistance	3.67Ω
Stator Voltage	415 volts	Rotor resistance	5.26 Ω
Stator Current	4.7 amps	Stator inductance	306.82 mH
Rotor Voltage	185 volts	Rotor inductance	306.82 mH
Rotor Current	7.5 amps	Magnetizing inductance	281.96 mH
Frequency			

References

[1] A. Vicenzutti, D. Bosich, G. Giadrossi, and G. Sulligoi, "The role of voltage controls in modern all-electric ships: Toward the all electric ship.," *IEEE Electrific. Mag.*, vol. 3, no. 2, pp. 49–65, Jun. 2015.

[2] G. Sulligoi, A. Vicenzutti, and R. Menis, "All-electric ship design: From electrical propulsion to integrated electrical and electronic power systems," *IEEE Trans. Transport. Electrific.*, vol. 2, no. 4, pp. 507–521, Dec. 2016.

[3] B. A. Kumar, K. A. Kumar, T. Radha, T. R. Chelliah, D. Khare, and U. S. Ramesh, "Control strategy for fuel saving in asynchronous generator driven electric tugboats," in *Proc. IEEE Sect. Int. Conf. Elect., Comput. Electron. Eng. (UPCON)*, Varanasi, India, Dec. 2016, pp. 467–472.

[4] A. J. Wasmund, "Series-versus parallel-connected generators (or multiple-engine D-C diesel-electric ship-propulsion systems," *Trans. Amer. Inst. Electr. Eng. II, Appl. Ind.*, vol. 73, no. 3, pp. 135–140, Jul. 1954.

[5] G. D. Proposta, "Operation of ships propellers," U.S. Patent 8 326 22A, Oct. 9, 1906.

[6] R. Borrás, R. Rodríguez, and M. Luace, "Starting of the naval diesel-electric propulsion. the vandal," *J. Maritime Res.*, vol. 8, no. 3, pp. 3–16, 2011.

[7] D. S. J. Seigne, "Marine electric propulsion," *Electr. Eng., Proc. Inst.*, vol. 111, no. 12, pp. 2060–2070, Dec. 1964.

[8] Gary. (2018). *Brief Look of Tugboat History, Harlow Marine International*. [Online]. Available: https://www.harlowmarine.com/a-brief-look-at-tugboat-history/

[9] N. T. Jucarone, "Electric propulsion for surface vessels," *Elect. Eng.*, vol. 67, no. 12, p. 1161, Dec. 1948.

[10] *Emission Standards: International: IMO Marine Engine Regulations*. [Online]. Available: https://www.dieselnet.com/standards/inter/imo.php AQ:7

[11] M. Mohammed Islam, "Power Generation and Distribution," in *Shipboard Power Systems Design and Verification Fundamentals*, vol. 1. Hoboken, NJ, USA: Wiley, 2018, p. 352.

[12] *Ships Electrical Standards, Revision 03*, document TP 127E, May 2018.

[13] L. L. J. Mahon, *Diesel Generator Handbook*. Oxford, U.K.: Butterworth-Heinemann, 1992.

[14] T. L. Vu, A. A. Ayu, J. S. Dhupia, L. Kennedy, and A. K. Adnanes, "Power management for electric tugboats through operating load estimation," *IEEE Trans. Control Syst. Technol.*, vol. 23, no. 6, pp. 2375–2382, Nov. 2015.

[15] B. A. Kumar, M. Chandrasekar, T. R. Chelliah, and U. S. Ramesh, "Fuel minimization in diesel-electric tugboat considering flywheel energy storage system," in *Proc. IEEE Transp. Electrific. Conf. Expo, Asia–Pacific (ITEC Asia–Pacific)*, Bangkok, Thailand, Jun. 2018, pp. 1–5.

[16] K. Satpathi, V. M. Balijepalli, and A. Ukil, "Modeling and real-time scheduling of DC platform supply vessel for fuel efficient operation," *IEEE Trans. Transport. Electrific.*, vol. 3, no. 3, pp. 762–778, Sep. 2017.

[17] M. Starke, L. M. Tolbert, and B. Ozpineci, "AC vs. DC distribution: A loss comparison," in *Proc. IEEE/PES Transmiss. Distrib. Conf. Expo.*, Chicago, IL, USA, Apr. 2008, pp. 1–7.

[18] J. F. Hansen and F. Wendt, "History and state of the art in commercial electric ship propulsion, integrated power systems, and future trends," *Proc. IEEE*, vol. 103, no. 12, pp. 2229–2242, Dec. 2015.

[19] S. Castellan, R. Menis, A. Tessarolo, F. Luise, and T. Mazzuca, "A review of power electronics equipment for all-electric ship MVDC power systems," *Int. J. Elect. Power Energy Syst.*, vol. 96, pp. 306–323, Mar. 2018.

[20] R. M. Calfo, J. A. Fulmer, and J. E. Tessaro, "Generators for use in electric marine ship propulsion systems," in *Proc. IEEE Power Eng. Soc. Summer Meeting,*, Chicago, IL, USA, vol. 1, Jul. 2002, pp. 254–259.

[21] E. A. Sciberras, B. Zahawi, D. J. Atkinson, A. Breijs, and J. H. van Vugt, "Managing shipboard energy: A stochastic approach special issue on marine systems electrification," *IEEE Trans. Transport. Electrific.*, vol. 2, no. 4, pp. 538–546, Dec. 2016.

[22] E. Skjong, T. A. Johansen, M. Molinas, and A. J. Sørensen, "Approaches to economic energy management in diesel-lectric marine vessels," *IEEE Trans. Transport. Electrific.*, vol. 3, no. 1, pp. 22–35, Mar. 2017.

[23] "Diesel generator efficiency curve for Ship-N417," Nisisiba Electric Co. Ltd., Himeji, Japan, Tech. Rep., Feb. 2011. AQ:8

[24] J. P. Trovão, F. Machado, and P. G. Pereirinha, "Hybrid electric excursion ships power supply system based on a multiple energy storage system," *IET Elect. Syst. Transp.*, vol. 6, no. 3, pp. 190–201, 2016.

[25] A. Dubey and S. Santoso, "Availability-based distribution circuit design for shipboard power system," *IEEE Trans. Smart Grid*, vol. 8, no. 4, pp. 1599–1608, Jul. 2017.

[26] T. V. Vu, D. Gonsoulin, F. Diaz, C. S. Edrington, and T. El-Mezyani, "Predictive control for energy management in ship power systems under high-power ramp rate loads," *IEEE Trans. Energy Convers*, vol. 32, no. 2, pp. 788–797, Jun. 2017.

[27] F. D. Kanellos, "Optimal power management with GHG emissions limitation in all-electric ship power systems comprising energy storage systems," *IEEE Trans. Power Syst.*, vol. 29, no. 1, pp. 330–339, Jan. 2014.

[28] T. Strasser, "A review of architectures and concepts for intelligence in future electric energy systems," *IEEE Trans. Ind. Electron.*, vol. 62, no. 4, pp. 2424–2438, Apr. 2015.

[29] S. G. Li, S. M. Sharkh, F. C. Walsh, and C. N. Zhang, "Energy and battery management of a plug-in series hybrid electric vehicle using fuzzy logic," *IEEE Trans. Veh. Technol.*, vol. 60, no. 8, pp. 3571–3585, Oct. 2011.

[30] H. Kanchev, D. Lu, F. Colas, V. Lazarov, and B. Francois, "Energy management and operational planning of a microgrid with a PV-based active generator for smart grid applications," *IEEE Trans. Ind. Electron.*, vol. 58, no. 10, pp. 4583–4592, Oct. 2011.

[31] N. Loganathan and K. Lakshmi, "Demand side energy management system using ANN based linear programming approach," in *Proc. IEEE Int. Conf. Comput. Intell. Res.*, Dec. 2014, pp. 1–5.

[32] S. Bashash, S. J. Moura, J. C. Forman, and H. K. Fathy, "Plug-in hybrid electric vehicle charge pattern optimization for energy cost and battery longevity," *J. Power Sour.*, vol. 196, no. 1, pp. 541–549, Jan. 2011.

[33] A. C. Luna, N. L. Diaz, M. Graells, J. C. Vasquez, and J. M. Guerrero, "Mixed-integer-linear-programming-based energy management system for hybrid PV-wind-battery microgrids: Modeling, design, and experimental verification," *IEEE Trans. Power Electron.*, vol. 32, no. 4, pp. 2769–2783, Apr. 2017.

[34] H. He, J. Zhang, and G. Li, "Model predictive control for energy management of a plug-in hybrid electric bus," *Energy Procedia*, vol. 88, pp. 901–907, Jun. 2016.

[35] T. I. Bø *et al.*, "Marine vessel and power plant system simulator," *IEEE Access*, vol. 3, pp. 2065–2079, 2015.

[36] T. I. Bø and T. A. Johansen, "Dynamic safety constraints by scenario-based economic model predictive control of marine electric power plants," *IEEE Trans. Transport. Electrific.*, vol. 3, no. 1, pp. 13–21, Mar. 2017.

[37] M. R. Banaei and R. Alizadeh, "Simulation-based modeling and power management of all-electric ships based on renewable energy generation using model predictive control strategy," *IEEE Intell. Transp. Syst. Mag.*, vol. 8, no. 2, pp. 90–103, Apr. 2016.

[38] P. Michalopoulos, F. D. Kanellos, G. J. Tsekouras, and J. M. Prousalidis, "A method for optimal operation of complex ship power systems employing shaft electric machines," *IEEE Trans. Transport. Electrific.*, vol. 2, no. 4, pp. 547–557, Dec. 2016.

[39] J. S. Dhupia, A. A. Ayu, and T. L. Vu, "Optimizing design and power management strategy of onboard DC grid based tugs," ABB Marines Cranes, Tech. Rep., 2014. AQ:9

[40] A. Joseph, K. Desingu, R. R. Semwal, T. R. Chelliah, and D. Khare, "Dynamic performance of pumping mode of 250 MW variable speed hydro-generating unit subjected to power and control circuit faults," *IEEE Trans. Energy Convers.*, vol. 33, no. 99, pp. 430–441, Mar. 2017.

[41] R. Pena, J. C. Clare, and G. M. Asher, "A doubly fed induction generator using back-to-back PWM converters supplying an isolated load from a variable speed wind turbine," *IEE Proc.-Electr. Power Appl.*, vol. 143, no. 5, pp. 380–387, Sep. 1996.

[42] G. LaLiberte and M. Kaderbhai, "The 10-second start NFPA 110 type 10 starting requirements for generator set applications," Tech. Rep., 2018. AQ:10

[43] A. Joseph, R. Selvaraj, T. R. Chelliah, and S. V. A. Sarma, "Starting and braking of a large variable speed hydrogenerating unit subjected to converter and sensor faults," *IEEE Trans. Ind Appl.*, vol. 54, no. 4, pp. 3372–3382, Jul/Aug. 2018.

[44] M. Koot, J. T. B. A. Kessels, B. de Jager, W. P. M. H. Heemels, P. P. J. van den Bosch, and M. Steinbuch, "Energy management strategies for vehicular electric power systems," *IEEE Trans. Veh. Technol.*, vol. 54, no. 3, pp. 771–782, May 2005.

[45] (2010). *Hybrid Shaft Generator Propulsion System Upgrade*. [Online]. Available: www.rolls-royce.com/~/media/Files/R/Rolls-Royce/../hsg-brochure.pdf

[46] Z. Zhou, M. B. Camara, and B. Dakyo, "Coordinated power control of variable-speed diesel generators and lithium-battery on a hybrid electric boat," *IEEE Trans. Veh. Technol.*, vol. 66, no. 7, pp. 5775–5784, Jul. 2017.

[47] S. Roy, O. P. Malik, and G. S. Hope, "A k-step predictive scheme for speed control of diesel driven power plants," in *Proc. Conf. Rec. IEEE Ind. Appl. Soc. Annu. Meeting*, Memphis, TN, USA, Oct. 1991, pp. 63–69.

[48] T. I. Bø. (2018). *Dynamic Model Predictive Control for Load Sharing in Electric Power Plants for Ships*. [Online]. Available: https://daim.idi.ntnu.no/masteroppgaver/007/7545/masteroppgave.pdf

[49] C. Yin, H. Wu, F. Locment, and M. Sechilariu, "Energy management of DC microgrid based on photovoltaic combined with diesel generator and supercapacitor," *Energy Convers. Manage.*, vol. 132, no. 15, pp. 14–27, Jan. 2017.

[50] B. Singh, G. Pathak, and B. K. Panigrahi, "Seamless transfer of renewable-based microgrid between utility grid and diesel generator," *IEEE Trans. Power Electron.*, vol. 33, no. 10, pp. 8427–8437, Oct. 2018.

[51] K. E. Yeager and J. R. Willis, "Modeling of emergency diesel generators in an 800 megawatt nuclear power plant," *IEEE Trans. Energy Convers.*, vol. 8, no. 3, pp. 433–441, Sep. 1993.

[52] R. Niwas and B. Singh, "Solid-state control for reactive power compensation and power quality improvement of wound field synchronous generator-based diesel generator sets," *IET Electr. Power Appl.*, vol. 9, no. 6, pp. 397–404, Jul. 2015.

[53] S. Benhamed *et al.*, "Dynamic modeling of diesel generator based on electrical and mechanical aspects," in *Proc. IEEE Elect. Power Energy Conf. (EPEC)*, Ottawa, ON, Canada, Oct. 2016, pp. 1–6.

[54] *550 kW Cummins Diesel Engine Generator/Standby/Electric Generator*. [Online]. Available: https://starlightgenerator.en.made-in-china.com/product/SCnJsBHXkLhj/China-550kw-Cummins-Diesel-Engine-Generator-Standby-Electric-Generator.html

[55] *1-2MW-Diesel-Generator*. [Online]. Available: https://laurel-generator.en.made-in-china.com/product/hCImNrvYHQcg/China-1500kVA-1-2MW-Diesel-Generator-Set.html

[56] R. Majumder, B. Chaudhuri, A. Ghosh, R. Majumder, G. Ledwich, and F. Zare, "Improvement of stability and load sharing in an autonomous microgrid using supplementary droop control loop," *IEEE Trans. Power Syst.*, vol. 25, no. 2, pp. 796–808, May 2010.

[57] E. A. Sciberras and R. A. Norman, "Multi-objective design of a hybrid propulsion system for marine vessels," *IET Electr. Syst. Transp.*, vol. 2, no. 3, pp. 148–157, Sep. 2012.

[58] C. Desai and S. S. Williamson, "Optimal design of a parallel hybrid electric vehicle using multi-objective genetic algorithms," in *Proc. IEEE Vehicle Power Propuls. Conf.*, Sep. 2009, pp. 871–876.

[59] K. N. Hasan, R. Preece, and J. V. Milanovic, "Priority ranking of critical uncertainties affecting small-disturbance stability using sensitivity analysis techniques," *IEEE Trans. Power Syst.*, vol. 32, no. 4, pp. 2629–2639, Jul. 2017.

[60] J. M. Holtzmann, "On using perturbation analysis to do sensitivity analysis: Derivatives versus differences," *IEEE Trans. Autom. Control*, vol. 37, no. 2, pp. 243–247, Feb. 1992.

Birudula Anil Kumar (S'16) received the bachelor's degree in electrical and electronics engineering from the Lakireddy Balireddy Engineering College, Mylavaram, India, in 2008, and the master's degree in power system from National Institute of Technology, Hamirpur, India, in 2012. He is currently pursuing the Ph.D. degree with the Hydropower Simulation Laboratory, Department of Water Resource Development and Management, IIT Roorkee, Roorkee, India.

From 2012 to 2014, he was an Assistant Professor with Lingayas University, Faridabad, India. His current research interests include hydroelectric systems and power optimization.

Raghu Selvaraj (S'14) received the bachelor's degree in electrical engineering from the Nandha Engineering College, Erode, India, in 2010, and the master's degree in power electronics and drives from SRM University, Chennai, India, in 2012. He is currently pursuing the Ph.D. degree with the Hydropower Simulation Laboratory, Department of Water Resource Development and Management, IIT Roorkee, Roorkee, India.

From 2012 to 2016, he was a Teaching Faculty with Marwadi University, Gujarat, India, NIT Calicut, Kozhikode, India, and SRM University. He has presented many research papers in various national and international conferences and journals. His current research interests include hydroelectric system, industrial drives, pulsewidth modulation techniques, and fault-tolerant operation of drives.

Thanga Raj Chelliah (S'06–M'11–SM'17) received the Diploma degree in electrical engineering from the Government Polytechnic College, Nagercoil, India, in 1996, the B.Eng. degree in electrical engineering from the Coimbatore Institute of Technology, Coimbatore, India, in 2002, the M.Eng. degree in electrical engineering from Anna University, Chennai, India, in 2005, and the Ph.D. degree in electrical engineering from IIT Roorkee, Roorkee, India, in 2009.

He has few years of industry experience, where has was involved energy conservation activities in electrical equipment. Since 2015, he has been with the Hydropower Simulation Laboratory, IIT Roorkee, where he is currently an Associate Professor with the Department of Water Resource Development and Management and an Officer-in-Charge of Hydropower Simulation, Power Electronics and Hydro-Electric Machines Laboratories. He has authored or co-authored a number of research papers in various journals and conferences of national and international repute. His current research interests include power electronics applications in large pumped storage plants, asynchronous generators, and marine propulsion systems.

Dr. Chelliah is a Senior Member of IEEE Industry Applications, Transportation Electrification, Power and Energy Societies, a Life Member of Indian Water Resources Society, and an Alternate Member of Hydroelectric Power House Structures Sectional Committee, Bureau of Indian Standards.

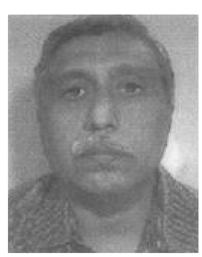

U.S. Ramesh completed the Directorate of Marine Engineering and Training in 1983. He joined the National Ship Design and Research Centre (NSDRC), Visakhapatnam, India, as a Manager, in 1996. He was involved in a number of design and research projects, especially in advanced technology areas such as ocean thermal energy conversion (OTEC), deep sea mining, and the National Data Buoy Program, National Institute of Ocean Technology. AQ:11 He was also involved in a number of design and research projects pertaining to ship design, ship construction, and marine engineering. He was the Chief Manager with Indian Maritime University, Visakhapatnam Campus. He has authored or co-authored a number of research papers in various journals and conferences of national and international repute. His current research interests include energy efficiency in maritime transport, ship design, and Marine Environmental protection.

Mr. Ramesh is a member of Joint Scientific and Technical Advisory Committee of Ministry of Earth Sciences, IEI (India), IMarE (India), and IMarest (U.K.), and the Technical Committee member of Indian Register of Shipping and Bureau of Indian Standards.